2020

Defining the border of the subthalamic nucleus for deep brain stimulation: A proposed model using the symmetrical sigmoid curve function

Anthony M.T Chau

Angela Jacques
The University of Notre Dame Australia, angela.jacques@nd.edu.au

Christopher R. Lind

This article was originally published as:
Chau, A. M., Jacques, A., & Lind, C. R. (2020). Defining the border of the subthalamic nucleus for deep brain stimulation: A proposed model using the symmetrical sigmoid curve function. *World Neurosurgery, Early View (Online First)*.

Original article available here:
https://doi.org/10.1016/j.wneu.2020.08.027

This is the accepted manuscript version of an article published as:

Chau, A.M.T., Jacques, A., and Lind, C.R. (2020) Defining the border of the subthalamic nucleus for deep brain stimulation: A proposed model using the symmetrical sigmoid curve function. *World Neurosurgery, Early View* (Online First).
https://doi.org/10.1016/j.wneu.2020.08.027

This article has been published in final form at https://doi.org/10.1016/j.wneu.2020.08.027

Defining the Border of the Subthalamic Nucleus for Deep Brain Stimulation: A Proposed Model Using the Symmetrical Sigmoid Curve Function

Anthony M.T. Chau[1], Angela Jacques[2], Christopher R. Lind[1,3]

BACKGROUND: **The subthalamic nucleus (STN) is an important target during deep brain stimulation (DBS). Accurate lead placement is integral to achieving satisfactory clinical outcomes; however, the STN remains a structure whose visualization is highly variable with borders often difficult to define. We aimed to develop an objective method of evaluating the visibility of the STN on preoperative magnetic resonance imaging (MRI) to standardize future comparative assessments between imaging protocols and patient-specific parameters.**

METHODS: **An imaging study of 64 prospectively collected patients undergoing bilateral DBS of the STN for various movement disorders was performed with institutional approval. MRI scans were acquired using a uniform protocol involving general anesthesia, cranial fixation in a Leksell stereotactic frame, and long acquisition times using a 3T MRI scanner. The images were analyzed using the iPlan Stereotaxy, version 2.6, workstation. High-resolution T2-weighted axial sections were evaluated, and the voxel values in the region of the presumed posterior border of the STN (as defined by the operating neurosurgeon) were obtained. A 4-parameter logistic symmetrical sigmoid curve was used to map the voxel values as they progressed from within to outside the region of the STN border. The inflection point and Hill coefficient of this symmetrical curve was calculated to provide objective information on the location and clarity of the STN border, respectively. These findings were compared with the surgeon's judgment of the STN border. To demonstrate the use of the sigmoid curve, the patients' head volumes were also calculated and evaluated to assess whether larger head volumes adversely affected STN visibility.**

RESULTS: **The symmetrical sigmoid curve model provided objective information on the visibility of the STN on T2-weighted MRI scans and could be generated in 86% of the patients. The other 14% of patients had MRI scans that generated linear graphs, indicating the poorest scoring for STN image quality. No correlation between head volume and STN visibility was identified.**

CONCLUSIONS: **Our proposed statistical model allows for standardized examination of the visibility of the STN border for DBS and has potential for both clinical and academic applications.**

INTRODUCTION

Stimulation of the subthalamic nucleus (STN), specifically its dorsolateral sensorimotor subdivision, is an effective treatment for a number of movement disorders. The success of surgery is reliant on accurate lead placement. Advances in magnetic resonance imaging (MRI) field strength to 3T has seen preoperative targeting gradually supersede atlas-based and intraoperative electrophysiological techniques.[1] As deep brain stimulation (DBS) groups have shifted toward using only direct anatomical identification for targeting and verifying the final lead placement, much of the current research efforts have focused on improving imaging protocols.

Key words
- Anthropometry
- Deep brain stimulation
- Magnetic resonance imaging
- Sigmoid curve
- Subthalamic nucleus

Abbreviations and Acronyms
CNR: Contrast/noise ratio
DBS: Deep brain stimulation
ET: Essential tremor
MRI: Magnetic resonance imaging
PD: Parkinson disease
STN: Subthalamic nucleus

From the [1]Department of Neurosurgery, Sir Charles Gairdner Hospital, Perth; [2]Institute for Health Research, University of Notre Dame, Fremantle; and [3]Faculty of Medical and Health Sciences, University of Western Australia, Perth, Western Australia, Australia

To whom correspondence should be addressed: Christopher R. Lind, M.B.B.S. [E-mail: Christopher.Lind@health.wa.gov.au]

Citation: World Neurosurg. (2020). https://doi.org/10.1016/j.wneu.2020.08.027

*Journal homepage: **www.journals.elsevier.com/world-neurosurgery***

*Available online: **www.sciencedirect.com***

1878-8750/$ - see front matter

However, the STN, estimated to be 3 × 5 × 12 mm in humans, remains a structure whose visualization has been highly variable, with borders often difficult to define.[2] This is in part because the posterior half of the STN has greater variation than the anterior half in its iron content and, hence, MRI signal characteristics.[3] Of most interest in our clinical practice has been the visual clarity of the posterior border of the STN when viewed in the axial plane, where it is located anterolateral to the red nucleus and separated by the medial forebrain bundle.[4] Confidence in the location of this posterior STN border is paramount in preoperative planning and achieving satisfactory clinical outcomes.

Comparative assessments of the visibility of the STN border in reported studies have evaluated different imaging modalities (e.g., T2-weighted imaging, susceptibility weighted imaging, quantitative susceptibility mapping). Similarly, assessments of patient-specific parameters that might influence the quality of the obtained images of the STN (e.g., age, brain volume, underlying pathology) have also been explored. However, without a standardized method for comparing these imaging datasets, it would be difficult to affirm which protocols or patient-specific parameters will lead to improved or poorer STN border visibility. Regions of interest measurements generating contrast/noise ratios (CNRs) do not fully convey this information because they indicate differences pertaining more to the center of adjacent structures rather than their borders. In addition, qualitative scores of STN visibility have been unsatisfactorily subjective.

Therefore, our primary aim in the present report was to describe a novel method with which to quantitatively assess the visibility of the border of the STN. We propose that multiple voxel values obtained along the border region from well within the STN to well outside of it can be graphed into a symmetrical sigmoid curve. Data from this function can then be used to objectify the location and clarity of the posterior STN border, providing quantitative and, in the future, reproducible data to allow for comparisons.

Second, it has been the clinical suspicion of the senior author (C.L.) that the definition of the STN border on T2-weighted MRI scans has been more challenging in patients with a larger head volume. Direct targeting operations have occasionally been aborted in favor of indirect methods when the STN could not be reliably identified on the preoperative planning T2-weighted MRI scan. Therefore, we aimed to use the sigmoid curve technique in an evaluation demonstration of whether larger head volumes would correlate with poorer definition of the posterior border of the STN on T2-weighted MRI scans.

METHODS

Stereotactic Technique

The imaging data from 64 consecutive patients during an 8-year period who had undergone bilateral DBS lead implantation for various movement disorders were evaluated. The imaging protocol was uniform, as previously described.[5] In brief, a Leksell stereotactic frame G (Elekta AB, Stockholm, Sweden) was positioned on the patient, general anesthesia was induced, and a preoperative 3T MRI scan using the Achieva 3.0 TX (Philips Healthcare, Amsterdam, Netherlands) with long acquisition times was obtained. T1-weighted volumetric data and high-resolution T2-weighted axial slices passing through the anterior commissure were obtained. The data were uploaded to an iPlan Stereotaxy, version 2.6, workstation (Brainlab, Munich, Germany), and preoperative planning was performed. The target STN was outlined on 3 contiguous axial T2-weighted slices with reference to the Schaltenbrand and Wahren[6] stereotactic atlas by the operating surgeon (C.L.).

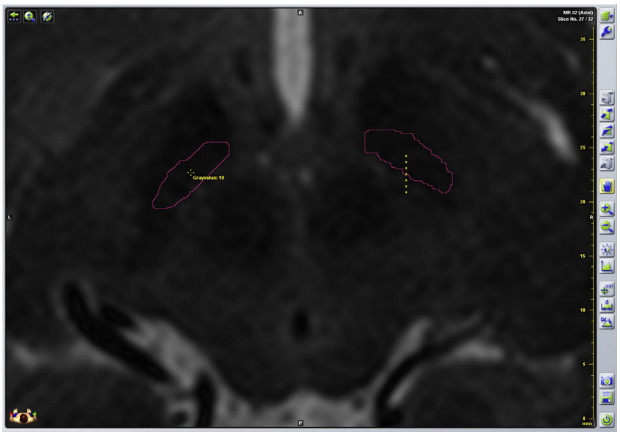

Figure 1. The subthalamic nucleus outlined by the surgeon (*pink*). Seven equidistant voxels spanning 4 mm and centered over the midpoint of the presumed posterior subthalamic nucleus border were evaluated for generation of the sigmoid curve.

Calculation of 4-Parameter Logistic Symmetrical Sigmoid Curve

The borders of the STN on 3 contiguous 1-mm T2-weighted axial sections, as defined by the operating neurosurgeon (C.L.), on the preoperative plan were examined. Voxel values beginning at the midpoint of the posterior border of the STN and proceeding in either direction were obtained. A total of 7 equidistant points were recorded over a 4-mm distance, centered at this posterior border (3 within the STN, 3 outside, and 1 at the border; Figure 1).

$$y = d + \frac{a - d}{1 + \left(\frac{x}{c}\right)^{b}}$$

Figure 2. The formula generated for the 4-parameter logistic sigmoid curve using a freely available online calculator (available at: www.mycurvefit.com) from the input of 7 data points: *a,* minimum asymptote (well within the subthalamic nucleus [STN]); *d,* maximum asymptote (well outside the STN, in the white matter); *c,* point of inflection (i.e., the STN border); *b,* Hill slope (i.e., steepness of the curve at the inflection point or STN border).

The data were entered into a freely available online calculator (available at: www.mycurvefit.com) and a symmetrical 4-parameter logistic sigmoid curve and its formula were generated (Figures 2 and 3). The data retrieved from this curve included the point of inflection, which provided an objective reference for the border within the measured 4-mm region. These data were then dichotomized to measure the accuracy of the surgeon's judgment of the location of the border to determine whether the border was different from the surgeon's impression (Table 1). If the data returned an inflection point outside the measured 4-mm range, the result was deemed a linear relationship (rather than a sigmoid curve)—indicating a poorly defined STN border.

Other data obtained from the sigmoid curve included the unitless Hill slope, which provided an objective reference for the crispness or delineation at the STN border. The steeper the slope at the point of inflection (i.e., the border), the higher the Hill slope, providing an objective indication of a crisper STN border definition. If the Hill slope returned a number (gradient) <3, the result was deemed a linear relationship (an indication of a poorly defined border).

To optimize the robustness of the voxel values and, therefore, the resultant sigmoid function, each patient had a total of 6 datasets obtained (right and left STN over 3 axial slices). The equivalent values were averaged to produce a single dataset and single sigmoid curve function for each patient.

Table 1. Scoring System to Compare the Objective Location of Subthalamic Nucleus Border with Surgeon's Impression

Category	Location of Inflection Point Relative to Surgeon's Plan	Interpretation
A	<0.5 mm	Surgeon's judgment of location of STN border correlated well with voxel values
B	>0.5 mm or a linear relationship	Border was poorly defined objectively

STN, subthalamic nucleus.

Calculation of Head Volume

The volume of the head was calculated from the preoperative volumetric T1-weighted MRI scan using the Brainlab software. The

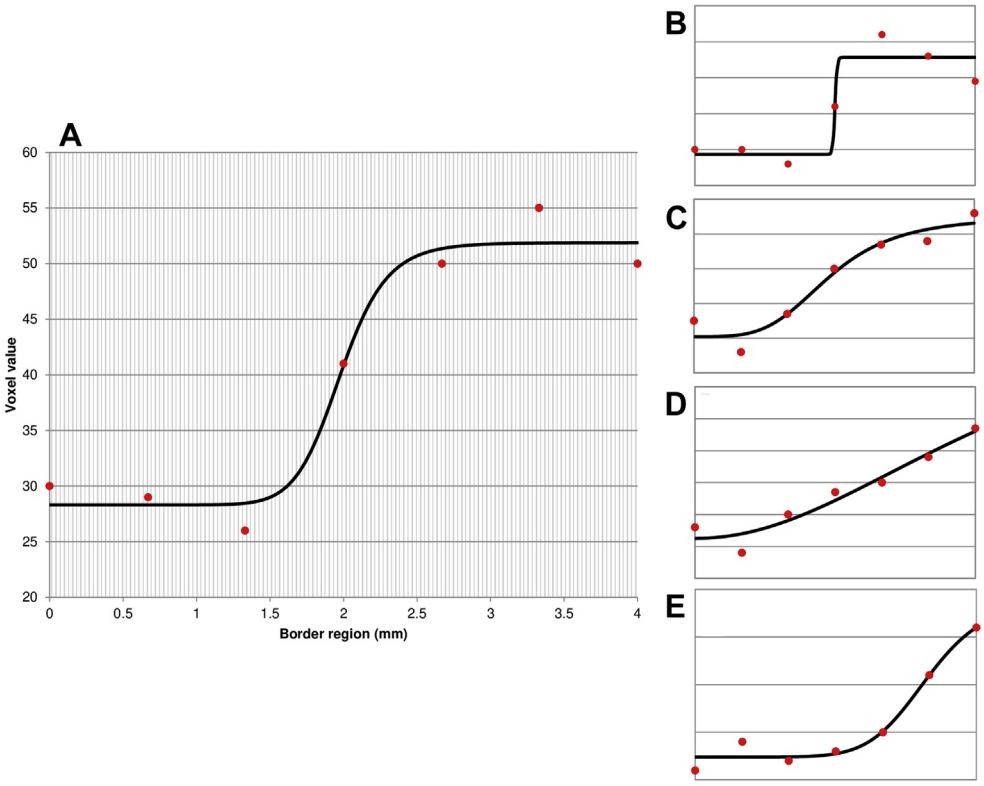

Figure 3. (**A**) The symmetrical 4-parameter logistic sigmoid curve automatically generated (calculator available at: www.mycurvefit.com) from the 7 voxels from the subthalamic nucleus border region. (**B**) A sigmoid curve with a high Hill slope showing a crisp border. (**C**) A sigmoid curve with a low Hill slope. (**D**) A linear graph, indicating that the border is ill-defined. (**E**) A sigmoid curve (inflection point) that had shifted (i.e., the border was not where the surgeon saw it).

volume of the scalp (not including the ears), skull, and intracranial contents from the level of the external auditory meatus upward (at the level of the floor of the middle fossa) were included (Figure 4).

Statistical Analysis

Descriptive statistics were based on frequency distributions for the categorical data and the mean ± standard deviations or median, interquartile range, and range for continuous data, depending on the distribution of the data. Categorical comparisons were based on patient factors, including age, sex, and diagnosis. Univariate analysis included 1-way analysis of variance and t tests for comparison of the mean head volumes between factor categories. Logistic regression was used to evaluate the association between an increasing head volume and the inflection point grades: category A (≤0.5 mm) compared with category B (>0.5 mm). Bivariate and partial (adjusting for sex) Pearson's product-moment correlations were used to determine whether any relationships existed between the head volume and Hill slope. The results were summarized as the β-coefficient and corresponding 95% confidence intervals. Statistical analysis was conducted using SPSS, version 25.0 (IBM Corp., Armonk, New York, USA) and Stata, version 15 (StataCorp, College Station, Texas, USA). All hypothesis tests were 2-sided, and P values <0.05 were considered statistically significant.

RESULTS

Study Population

A total of 64 consecutive patients with an average age of 60.1 ± 10.7 years (range, 21–79 years) had undergone bilateral DBS implantation for various movement disorders: 44 for Parkinson disease (PD), 16 for essential tremor (ET), 3 for both PD and ET, and 1 for generalized dystonia (Table 2). Of the 64 patients, 44 were men and 20 were women. The mean head volume was 2737 ± 270 cm^3 (range, 2185–3244 cm^3). Because the male head volume was significantly larger than the female head volume ($P < 0.001$), the subsequent statistical analysis assessing the inflection point and Hill slope included an adjustment for sex.

Patients consented to be part of the research project under the approval of the Sir Charles Gairdner Hospital clinical ethics committee (reference numbers 2009-145 and 2012-039).

Head Volume Versus Inflection Point (Category A vs. Category B)

After adjustment for sex, no association was found between the head volume and inflection point categories (odds ratio, 0.99; 95% confidence interval, 0.99–1.00; $P = 0.593$; Figure 5).

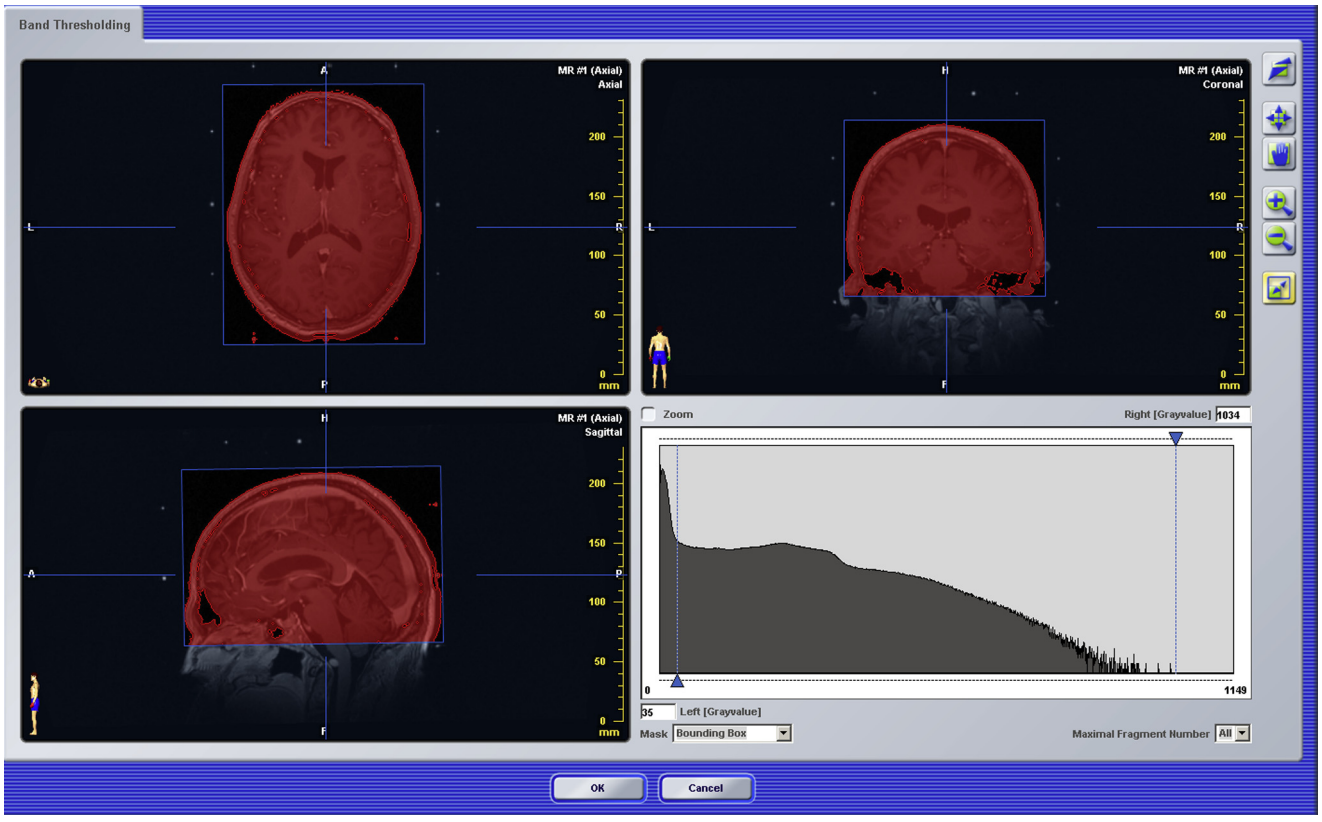

Figure 4. The head volume was calculated using the stereotactic Brainlab software.

Table 2. Demographic Data and Results

Characteristic	Patients	Head Volume (cm^3)	*P* Value
Diagnosis			0.375
ET	16 (25.0)	2757 ± 272	
GD	1 (1.6)	2293	
PD	44 (68.8)	2733 ± 264	
PD + ET	3 (4.7)	2832 ± 360	
Sex			<0.001
Female	20 (31.3)	2478 ± 190	
Male	44 (68.8)	2855 ± 214	
Age (years)			0.155
≤60	28 (43.8)	2792 ± 261	
>60	36 (56.3)	2694 ± 273	
Inflection point score			0.252
A (≤0.5 mm)	38 (59.4)	2705 ± 279	
B (>0.5 mm)	26 (40.6)	2784 ± 255	
Sigmoid curve generated			0.942
Yes	55 (85.9)	2738 ± 269	
No (linear)	9 (14.1)	2731 ± 263	

Data presented as *n* (%) or mean ± standard deviation.
ET, essential tremor; GD, generalized dystonia; PD, Parkinson disease.

Head Volume Versus Hill Slope

The average Hill slope was 6.2 (interquartile range, 3.5–8.9; range, 1–119). No statistically significant bivariate correlation ($r = -0.011$; $P = 0.929$) or partial correlation, after adjustment for sex ($r = 0.021$; $P = 0.880$), was found (Figure 6). Of the 64 patients, 14% demonstrated a "linear" relationship at the border region, indicating the poorest score for visualization of the STN. The diagnoses for these patients were PD in 5 patients, ET in 3 patients, and both PD and ET in 1 patient. No statistically significant difference was found between the head volumes of these patients and those with a sigmoid curve at the STN border ($P = 0.942$).

DISCUSSION

Sigmoid Curve

The Hill equation was first reported in 1910 to describe the relationship between oxygen tension and hemoglobin saturation. It has since been widely used to describe many nonlinear, saturable processes in physiology, biochemistry, and pharmacodynamics. Common examples include modeling ligand–receptor binding and the dose–response relationship of a drug. The 4-parameter logistic Hill equation is a regression model with a sigmoid shape, composed of 4 variables: a, the minimum asymptote; d, the maximum asymptote; c, the inflection point; and b, the maximum slope (which occurs at the inflection point; Figure 2).

This 4-parameter logistic curve is based on the assumption that the data will be symmetrical around its midpoint (inflection point). This is a reasonably fair assumption when applied to the STN model. On T2-weighted MRI scans, the STN will be hypointense owing to the high iron content, and the surrounding tissue with a low iron content will be relatively hyperintense. Using the method we have described, 1 asymptote of the sigmoid curve will be well within the posterior STN and the other will be well outside of it. The STN border will be within the prescribed 4-mm border region, and the voxel data provide objective information on the inflection point (border location) and Hill slope (a measure of the abruptness or clarity of this border). When the

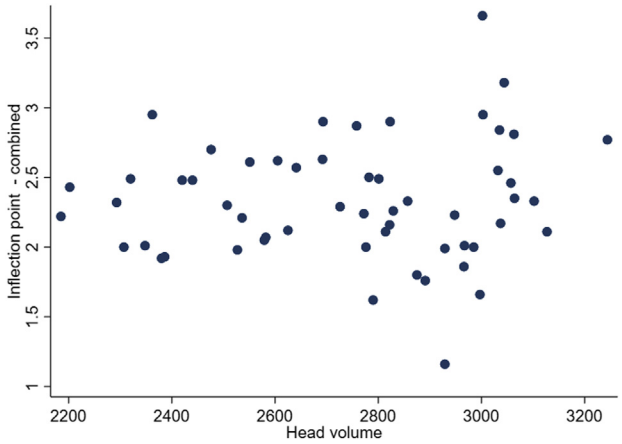

Figure 5. Scatterplot of the head volume versus the inflection point (subthalamic nucleus [STN] border location). The surgeon's judgment of the location of the STN border within the allocated 4-mm measured region was at 2 mm; the *dots* represent the objective measurements of the border location. Some dots outside the region of 0–4 mm (from magnetic resonance imaging scans with linear graphs; $n = 9$) were not depicted in this visual representation. No statistically significant difference was found between the accuracy of the surgeon's judgment of the STN border location and an increasing head volume.

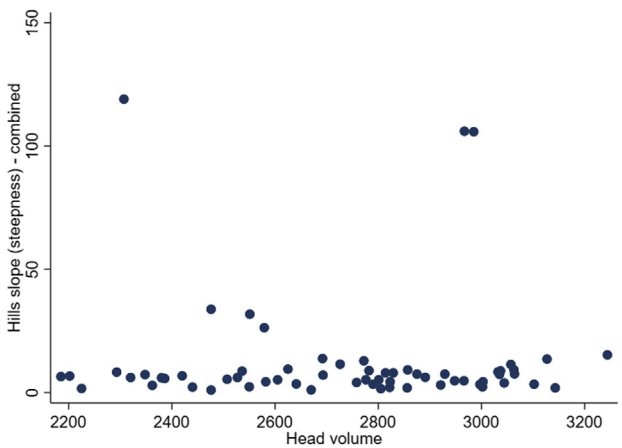

Figure 6. Scatterplot of the head volume versus the Hill slope (subthalamic nucleus border clarity). No statistically significant difference was found between an increasing head volume and changes in the Hill slope.

Table 3. Summary of Existing Qualitative Assessment Methods

Investigator	Method
Dimov et al.,[7] 2018	5-Point scale: 0 (STN border not visible) to 4 (all borders clearly defined, with an intensity gradient along the STN toward its caudal pole visible)
Ranjan et al.,[8] 2018	4-Point scale: 0 (STN border not visible) to 3 (excellent, with STN boundary visible and definitely clear)
Nagahama et al.,[9] 2015	4-Point scale: 0 (STN border not visible) to 3 (excellent, with STN boundary visible and definitely clear)
Liu et al.,[10] 2013	4-Point scale: 0 (STN border not visible) to 3 (STN well-defined and clearly differentiated from its superior neighbor [ZI] and inferior neighbor [SN])

STN, subthalamic nucleus; ZI, zona incerta; SN, substantia nigra.

border is poorly defined, a line, rather than a sigmoid curve, will be generated.

Comparison with Other Visualization Scores

Our method provides a novel and simple quantitative assessment of the quality or usability of an MRI scan for the visualization of the STN for DBS, providing an objective measure of the STN border location and clarity. Previous groups have described qualitative assessment of the STN and its borders using ordinal scales (Table 3).[7-10] However, the subjective nature of these scales has been a major shortcoming that could impair reliable replication by other investigators.

Quantitative assessment of the visibility of the STN has also been described using CNRs. The mean intensity value of voxels within a nominated STN region of interest is compared with the mean value of voxels of the surrounding tissue and set against various definitions of image noise (Table 4).[7,9-11] These offer an improved objective method; however, the interpretation is not particularly intuitive and the definition of CNR has varied in reported studies. Furthermore, the values provide a measure of the mean contrast of a structure relative to its neighbor, rather than specific information of the contrast at the border, which is the region of most interest to DBS surgeons.

Table 4. Summary of Existing Quantitative Assessment Methods

Investigator	Method
Dimov et al.,[7] 2018	CNR: $(ROI_{STN} - ROI_{WM})/SD_{WM}$ (STN divided into quadrants, with signal intensity measured within a ROI inside and outside the STN, divided by the SD of the intensity within the adjacent WM)
Alkemade et al.,[11] 2017	CNR: $(ROI_{inside\ STN} - ROI_{outside\ STN})/SD_{outside\ STN}$
Nagahama et al.,[9] 2015	CNR: $(ROI_{STN} - ROI_{SN})/SD_{STN}$ (coronal imaging used)
Liu et al.,[10] 2013	CNR: $(ROI_{inside\ STN} - ROI_{outside\ STN})/SD_{thalamus}$

CNR, contrast/noise ratio; ROI, region of interest; STN, subthalamic nucleus; WM, (adjacent) white matter; SD, standard deviation; SN, substantia nigra.

Application of Sigmoid Function Technique

Use of the sigmoid curve in the present report demonstrated that a larger head volume (measuring the supratentorial compartment, including the skull and scalp) did not result in poorer visualization of the STN. Until now, according to our literature search, no other study has specifically addressed such a hypothesis. The closest study was reported by Ranjan et al.,[8] who found that a lower volume of white matter correlated with poorer STN visualization using fast spin echo inversion recovery MRI. White matter atrophy correlates with age. Also, other studies have reported that the STN volume and neuron count will decline with age[12]; thus, this observation was related to a different clinical phenomenon. It is an interesting observation, nevertheless, because it is apparently in contrast to intuition from the reported data, which have documented a progressive increase in the iron concentration in other nuclei of the basal ganglia (and, therefore, presumably better delineation on T2-weighted MRI).[3]

Understanding the factors affecting visualization could support future research and guide imaging advances. On a day-to-day basis, it might also prompt the neurosurgeon in the preoperative setting, especially one who relies wholly on image guidance, to consider other targeting methods or to choose a different DBS target in the appropriate setting, such as the globus pallidus interna or the ventral intermedius nucleus. Although in our study, the sigmoid curve was determined with reference to the surgeon's judgment of the border location, the corollary is also possible during preoperative planning (i.e., if an STN border appears indistinct, voxels taken along the border region could be graphed to aid in a best estimate of its location). Although the sigmoid function method described in our concept study was not used to map the posterior STN border preoperatively per se, future studies in which the technique is primarily used should consider incorporating a method to assess and verify final lead placement accuracy (e.g., through correlation with clinical response).

CONCLUSION

Similar to other quantitative tools, the novel application of the sigmoid curve function allows for an objective assessment and, therefore, comparison of MRI scans for DBS. It is conceptually simple with potential utility in both the clinical and the academic setting. We used the sigmoid curve to demonstrate that the head volume does not adversely affect STN image quality on high-resolution T2-weighted MRI scans.

CRediT AUTHORSHIP CONTRIBUTION STATEMENT

Anthony M.T. Chau: Conceptualization, Methodology, Investigation, Formal analysis, Writing - original draft, Writing - review & editing, Visualization. **Angela Jacques:** Formal analysis, Visualization. **Christopher R. Lind:** Conceptualization, Methodology, Resources, Writing - review & editing, Supervision.

ACKNOWLEDGMENTS

The authors thank Professor Max K. Bulsara, Chair, Department of Biostatistics, University of Notre Dame, for his advice.

REFERENCES

1. Kocabicak E, Alptekin O, Ackermans L, et al. Is there still need for microelectrode recording now the subthalamic nucleus can be well visualized with high field and ultrahigh MR imaging? *Front Integr Neurosci*. 2015;9:46.

2. Yelnik J. Functional anatomy of the basal ganglia. *Mov Disord*. 2002;17:S15-S21.

3. Dormont D, Ricciardi KG, Tande D, et al. Is the subthalamic nucleus hypointense on T2-weighted images? A correlation study using MR imaging and stereotactic atlas data. *AJNR Am J Neuroradiol*. 2004;25:1516-1523.

4. Güngör A, Baydin ŞS, Holanda VM, et al. Microsurgical anatomy of the subthalamic nucleus: correlating fiber dissection results with 3-T magnetic resonance imaging using neuronavigation. *J Neurosurg*. 2018;130:716-732.

5. Thani NB, Bala A, Lind CR. Accuracy of magnetic resonance imaging-directed frame-based stereotaxis. *Neurosurgery*. 2012;70:114-123.

6. Schaltenbrand G, Wahren W. *Atlas for Stereotaxy of the Human Brain*. New York, NY: Thieme Medical Publishers; 1977.

7. Dimov AV, Gupta A, Kopell BH, Wang Y. High-resolution QSM for functional and structural depiction of subthalamic nuclei in DBS presurgical mapping. *J Neurosurg*. 2018;131:360-367.

8. Ranjan M, Boutet A, Xu DS, et al. Subthalamic nucleus visualization on routine clinical preoperative MRI scans: a retrospective study of clinical and image characteristics predicting its visualization. *Stereotact Funct Neurosurg*. 2018;96:120-126.

9. Nagahama H, Suzuki K, Shonai T, et al. Comparison of magnetic resonance imaging sequences for depicting the subthalamic nucleus for deep brain stimulation. *Radiol Phys Technol*. 2015;8:30-35.

10. Liu T, Eskreis-Winkler S, Schweitzer AD, et al. Improved subthalamic nucleus depiction with quantitative susceptibility mapping. *Radiology*. 2013;269:216-226.

11. Alkemade A, de Hollander G, Keuken MC, et al. Comparison of T2*-weighted and QSM contrasts in Parkinson's disease to visualize the STN with MRI. *PLoS One*. 2017;12:e0176130.

12. Zwirner J, Mobius D, Bechmann I, et al. Subthalamic nucleus volumes are highly consistent but decrease age-dependently—a combined magnetic resonance imaging and stereology approach in humans. *Hum Brain Mapp*. 2017;38:909-922.

Conflict of interest statement: The authors declare that the article content was composed in the absence of any commercial or financial relationships that could be construed as a potential conflict of interest.

Received 7 July 2020; accepted 3 August 2020

Citation: World Neurosurg. (2020). https://doi.org/10.1016/j.wneu.2020.08.027

*Journal homepage: **www.journals.elsevier.com/world-neurosurgery***

*Available online: **www.sciencedirect.com***

Defining the Border of the Subthalamic Nucleus for Deep Brain Stimulation: A Proposed Model Using the Symmetrical Sigmoid Curve Function

Anthony M.T. Chau[1], Angela Jacques[2], Christopher R. Lind[1,3]

BACKGROUND: **The subthalamic nucleus (STN) is an important target during deep brain stimulation (DBS). Accurate lead placement is integral to achieving satisfactory clinical outcomes; however, the STN remains a structure whose visualization is highly variable with borders often difficult to define. We aimed to develop an objective method of evaluating the visibility of the STN on preoperative magnetic resonance imaging (MRI) to standardize future comparative assessments between imaging protocols and patient-specific parameters.**

METHODS: **An imaging study of 64 prospectively collected patients undergoing bilateral DBS of the STN for various movement disorders was performed with institutional approval. MRI scans were acquired using a uniform protocol involving general anesthesia, cranial fixation in a Leksell stereotactic frame, and long acquisition times using a 3T MRI scanner. The images were analyzed using the iPlan Stereotaxy, version 2.6, workstation. High-resolution T2-weighted axial sections were evaluated, and the voxel values in the region of the presumed posterior border of the STN (as defined by the operating neurosurgeon) were obtained. A 4-parameter logistic symmetrical sigmoid curve was used to map the voxel values as they progressed from within to outside the region of the STN border. The inflection point and Hill coefficient of this symmetrical curve was calculated to provide objective information on the location and clarity of the STN border, respectively. These findings were compared with the surgeon's judgment of the STN border. To demonstrate the use of the sigmoid curve, the patients' head volumes were also calculated and evaluated to assess whether larger head volumes adversely affected STN visibility.**

RESULTS: **The symmetrical sigmoid curve model provided objective information on the visibility of the STN on T2-weighted MRI scans and could be generated in 86% of the patients. The other 14% of patients had MRI scans that generated linear graphs, indicating the poorest scoring for STN image quality. No correlation between head volume and STN visibility was identified.**

CONCLUSIONS: **Our proposed statistical model allows for standardized examination of the visibility of the STN border for DBS and has potential for both clinical and academic applications.**

INTRODUCTION

Stimulation of the subthalamic nucleus (STN), specifically its dorsolateral sensorimotor subdivision, is an effective treatment for a number of movement disorders. The success of surgery is reliant on accurate lead placement. Advances in magnetic resonance imaging (MRI) field strength to 3T has seen preoperative targeting gradually supersede atlas-based and intraoperative electrophysiological techniques.[1] As deep brain stimulation (DBS) groups have shifted toward using only direct anatomical identification for targeting and verifying the final lead placement, much of the current research efforts have focused on improving imaging protocols.

Key words
- Anthropometry
- Deep brain stimulation
- Magnetic resonance imaging
- Sigmoid curve
- Subthalamic nucleus

Abbreviations and Acronyms
CNR: Contrast/noise ratio
DBS: Deep brain stimulation
ET: Essential tremor
MRI: Magnetic resonance imaging
PD: Parkinson disease
STN: Subthalamic nucleus

From the [1]Department of Neurosurgery, Sir Charles Gairdner Hospital, Perth; [2]Institute for Health Research, University of Notre Dame, Fremantle; and [3]Faculty of Medical and Health Sciences, University of Western Australia, Perth, Western Australia, Australia

To whom correspondence should be addressed: Christopher R. Lind, M.B.B.S. [E-mail: Christopher.Lind@health.wa.gov.au]

Citation: World Neurosurg. (2020). https://doi.org/10.1016/j.wneu.2020.08.027

*Journal homepage: **www.journals.elsevier.com/world-neurosurgery***

*Available online: **www.sciencedirect.com***

1878-8750/$ - see front matter

However, the STN, estimated to be 3 × 5 × 12 mm in humans, remains a structure whose visualization has been highly variable, with borders often difficult to define.[2] This is in part because the posterior half of the STN has greater variation than the anterior half in its iron content and, hence, MRI signal characteristics.[3] Of most interest in our clinical practice has been the visual clarity of the posterior border of the STN when viewed in the axial plane, where it is located anterolateral to the red nucleus and separated by the medial forebrain bundle.[4] Confidence in the location of this posterior STN border is paramount in preoperative planning and achieving satisfactory clinical outcomes.

Comparative assessments of the visibility of the STN border in reported studies have evaluated different imaging modalities (e.g., T2-weighted imaging, susceptibility weighted imaging, quantitative susceptibility mapping). Similarly, assessments of patient-specific parameters that might influence the quality of the obtained images of the STN (e.g., age, brain volume, underlying pathology) have also been explored. However, without a standardized method for comparing these imaging datasets, it would be difficult to affirm which protocols or patient-specific parameters will lead to improved or poorer STN border visibility. Regions of interest measurements generating contrast/noise ratios (CNRs) do not fully convey this information because they indicate differences pertaining more to the center of adjacent structures rather than their borders. In addition, qualitative scores of STN visibility have been unsatisfactorily subjective.

Therefore, our primary aim in the present report was to describe a novel method with which to quantitatively assess the visibility of the border of the STN. We propose that multiple voxel values obtained along the border region from well within the STN to well outside of it can be graphed into a symmetrical sigmoid curve. Data from this function can then be used to objectify the location and clarity of the posterior STN border, providing quantitative and, in the future, reproducible data to allow for comparisons.

Second, it has been the clinical suspicion of the senior author (C.L.) that the definition of the STN border on T2-weighted MRI scans has been more challenging in patients with a larger head volume. Direct targeting operations have occasionally been aborted in favor of indirect methods when the STN could not be reliably identified on the preoperative planning T2-weighted MRI scan. Therefore, we aimed to use the sigmoid curve technique in an evaluation demonstration of whether larger head volumes would correlate with poorer definition of the posterior border of the STN on T2-weighted MRI scans.

METHODS

Stereotactic Technique

The imaging data from 64 consecutive patients during an 8-year period who had undergone bilateral DBS lead implantation for various movement disorders were evaluated. The imaging protocol was uniform, as previously described.[5] In brief, a Leksell stereotactic frame G (Elekta AB, Stockholm, Sweden) was positioned on the patient, general anesthesia was induced, and a preoperative 3T MRI scan using the Achieva 3.0 TX (Philips Healthcare, Amsterdam, Netherlands) with long acquisition times was obtained. T1-weighted volumetric data and high-resolution T2-weighted axial slices passing through the anterior commissure were obtained. The data were uploaded to an iPlan Stereotaxy, version 2.6, workstation (Brainlab, Munich, Germany), and preoperative planning was performed. The target STN was outlined on 3 contiguous axial T2-weighted slices with reference to the Schaltenbrand and Wahren[6] stereotactic atlas by the operating surgeon (C.L.).

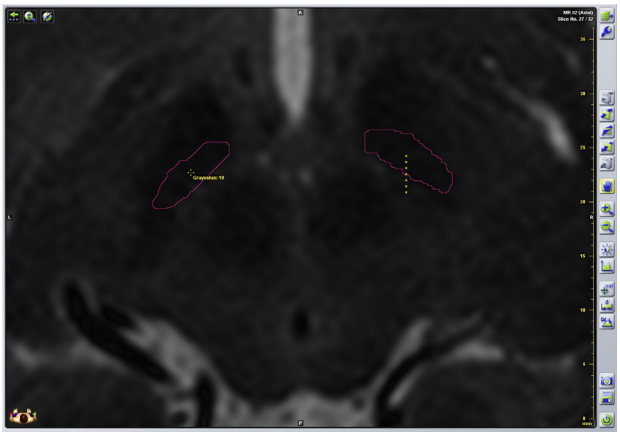

Figure 1. The subthalamic nucleus outlined by the surgeon (*pink*). Seven equidistant voxels spanning 4 mm and centered over the midpoint of the presumed posterior subthalamic nucleus border were evaluated for generation of the sigmoid curve.

Calculation of 4-Parameter Logistic Symmetrical Sigmoid Curve

The borders of the STN on 3 contiguous 1-mm T2-weighted axial sections, as defined by the operating neurosurgeon (C.L.), on the preoperative plan were examined. Voxel values beginning at the midpoint of the posterior border of the STN and proceeding in either direction were obtained. A total of 7 equidistant points were recorded over a 4-mm distance, centered at this posterior border (3 within the STN, 3 outside, and 1 at the border; Figure 1).

$$y = d + \frac{a - d}{1 + \left(\frac{x}{c}\right)^{b}}$$

Figure 2. The formula generated for the 4-parameter logistic sigmoid curve using a freely available online calculator (available at: www.mycurvefit.com) from the input of 7 data points: *a,* minimum asymptote (well within the subthalamic nucleus [STN]); *d,* maximum asymptote (well outside the STN, in the white matter); *c,* point of inflection (i.e., the STN border); *b,* Hill slope (i.e., steepness of the curve at the inflection point or STN border).

The data were entered into a freely available online calculator (available at: www.mycurvefit.com) and a symmetrical 4-parameter logistic sigmoid curve and its formula were generated (Figures 2 and 3). The data retrieved from this curve included the point of inflection, which provided an objective reference for the border within the measured 4-mm region. These data were then dichotomized to measure the accuracy of the surgeon's judgment of the location of the border to determine whether the border was different from the surgeon's impression (Table 1). If the data returned an inflection point outside the measured 4-mm range, the result was deemed a linear relationship (rather than a sigmoid curve)—indicating a poorly defined STN border.

Other data obtained from the sigmoid curve included the unitless Hill slope, which provided an objective reference for the crispness or delineation at the STN border. The steeper the slope at the point of inflection (i.e., the border), the higher the Hill slope, providing an objective indication of a crisper STN border definition. If the Hill slope returned a number (gradient) <3, the result was deemed a linear relationship (an indication of a poorly defined border).

To optimize the robustness of the voxel values and, therefore, the resultant sigmoid function, each patient had a total of 6 datasets obtained (right and left STN over 3 axial slices). The equivalent values were averaged to produce a single dataset and single sigmoid curve function for each patient.

Table 1. Scoring System to Compare the Objective Location of Subthalamic Nucleus Border with Surgeon's Impression

Category	Location of Inflection Point Relative to Surgeon's Plan	Interpretation
A	<0.5 mm	Surgeon's judgment of location of STN border correlated well with voxel values
B	>0.5 mm or a linear relationship	Border was poorly defined objectively

STN, subthalamic nucleus.

Calculation of Head Volume

The volume of the head was calculated from the preoperative volumetric T1-weighted MRI scan using the Brainlab software. The

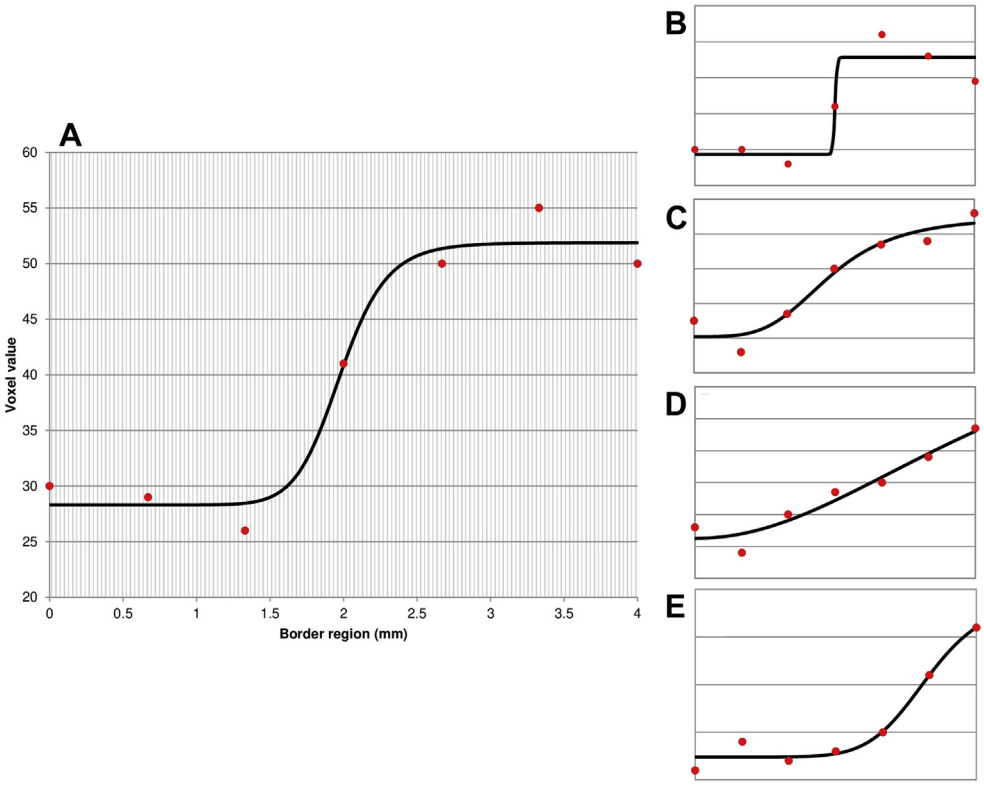

Figure 3. (**A**) The symmetrical 4-parameter logistic sigmoid curve automatically generated (calculator available at: www.mycurvefit.com) from the 7 voxels from the subthalamic nucleus border region. (**B**) A sigmoid curve with a high Hill slope showing a crisp border. (**C**) A sigmoid curve with a low Hill slope. (**D**) A linear graph, indicating that the border is ill-defined. (**E**) A sigmoid curve (inflection point) that had shifted (i.e., the border was not where the surgeon saw it).

volume of the scalp (not including the ears), skull, and intracranial contents from the level of the external auditory meatus upward (at the level of the floor of the middle fossa) were included (Figure 4).

Statistical Analysis

Descriptive statistics were based on frequency distributions for the categorical data and the mean ± standard deviations or median, interquartile range, and range for continuous data, depending on the distribution of the data. Categorical comparisons were based on patient factors, including age, sex, and diagnosis. Univariate analysis included 1-way analysis of variance and t tests for comparison of the mean head volumes between factor categories. Logistic regression was used to evaluate the association between an increasing head volume and the inflection point grades: category A (≤0.5 mm) compared with category B (>0.5 mm). Bivariate and partial (adjusting for sex) Pearson's product-moment correlations were used to determine whether any relationships existed between the head volume and Hill slope. The results were summarized as the β-coefficient and corresponding 95% confidence intervals. Statistical analysis was conducted using SPSS, version 25.0 (IBM Corp., Armonk, New York, USA) and Stata, version 15 (StataCorp, College Station, Texas, USA). All hypothesis tests were 2-sided, and P values <0.05 were considered statistically significant.

RESULTS

Study Population

A total of 64 consecutive patients with an average age of 60.1 ± 10.7 years (range, 21–79 years) had undergone bilateral DBS implantation for various movement disorders: 44 for Parkinson disease (PD), 16 for essential tremor (ET), 3 for both PD and ET, and 1 for generalized dystonia (Table 2). Of the 64 patients, 44 were men and 20 were women. The mean head volume was 2737 ± 270 cm^3 (range, 2185–3244 cm^3). Because the male head volume was significantly larger than the female head volume ($P < 0.001$), the subsequent statistical analysis assessing the inflection point and Hill slope included an adjustment for sex.

Patients consented to be part of the research project under the approval of the Sir Charles Gairdner Hospital clinical ethics committee (reference numbers 2009-145 and 2012-039).

Head Volume Versus Inflection Point (Category A vs. Category B)

After adjustment for sex, no association was found between the head volume and inflection point categories (odds ratio, 0.99; 95% confidence interval, 0.99–1.00; $P = 0.593$; Figure 5).

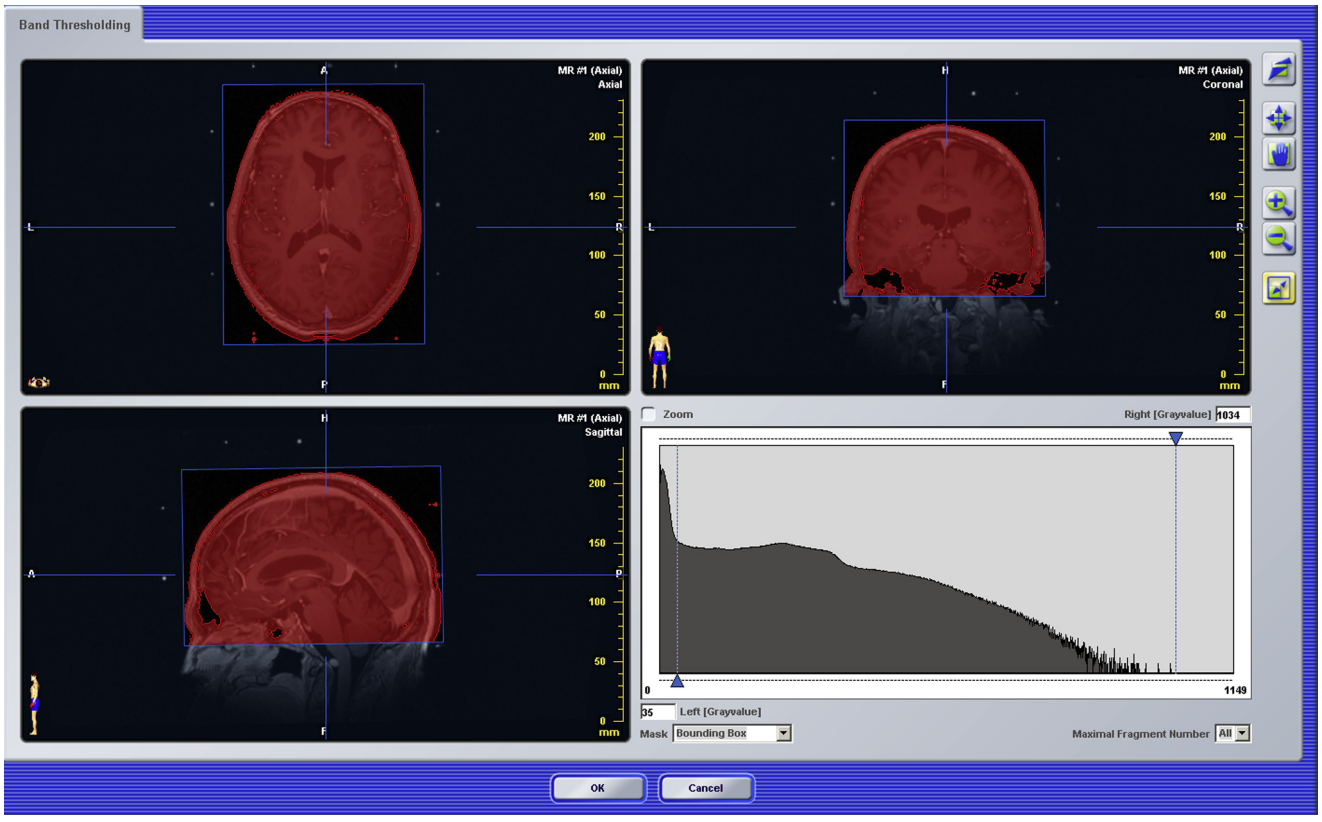

Figure 4. The head volume was calculated using the stereotactic Brainlab software.

Table 2. Demographic Data and Results

Characteristic	Patients	Head Volume (cm^3)	*P* Value
Diagnosis			0.375
ET	16 (25.0)	2757 ± 272	
GD	1 (1.6)	2293	
PD	44 (68.8)	2733 ± 264	
PD + ET	3 (4.7)	2832 ± 360	
Sex			<0.001
Female	20 (31.3)	2478 ± 190	
Male	44 (68.8)	2855 ± 214	
Age (years)			0.155
≤60	28 (43.8)	2792 ± 261	
>60	36 (56.3)	2694 ± 273	
Inflection point score			0.252
A (≤0.5 mm)	38 (59.4)	2705 ± 279	
B (>0.5 mm)	26 (40.6)	2784 ± 255	
Sigmoid curve generated			0.942
Yes	55 (85.9)	2738 ± 269	
No (linear)	9 (14.1)	2731 ± 263	

Data presented as *n* (%) or mean ± standard deviation.
ET, essential tremor; GD, generalized dystonia; PD, Parkinson disease.

Head Volume Versus Hill Slope

The average Hill slope was 6.2 (interquartile range, 3.5–8.9; range, 1–119). No statistically significant bivariate correlation ($r = -0.011$; $P = 0.929$) or partial correlation, after adjustment for sex ($r = 0.021$; $P = 0.880$), was found (Figure 6). Of the 64 patients, 14% demonstrated a "linear" relationship at the border region, indicating the poorest score for visualization of the STN. The diagnoses for these patients were PD in 5 patients, ET in 3 patients, and both PD and ET in 1 patient. No statistically significant difference was found between the head volumes of these patients and those with a sigmoid curve at the STN border ($P = 0.942$).

DISCUSSION

Sigmoid Curve

The Hill equation was first reported in 1910 to describe the relationship between oxygen tension and hemoglobin saturation. It has since been widely used to describe many nonlinear, saturable processes in physiology, biochemistry, and pharmacodynamics. Common examples include modeling ligand–receptor binding and the dose–response relationship of a drug. The 4-parameter logistic Hill equation is a regression model with a sigmoid shape, composed of 4 variables: a, the minimum asymptote; d, the maximum asymptote; c, the inflection point; and b, the maximum slope (which occurs at the inflection point; Figure 2).

This 4-parameter logistic curve is based on the assumption that the data will be symmetrical around its midpoint (inflection point). This is a reasonably fair assumption when applied to the STN model. On T2-weighted MRI scans, the STN will be hypointense owing to the high iron content, and the surrounding tissue with a low iron content will be relatively hyperintense. Using the method we have described, 1 asymptote of the sigmoid curve will be well within the posterior STN and the other will be well outside of it. The STN border will be within the prescribed 4-mm border region, and the voxel data provide objective information on the inflection point (border location) and Hill slope (a measure of the abruptness or clarity of this border). When the

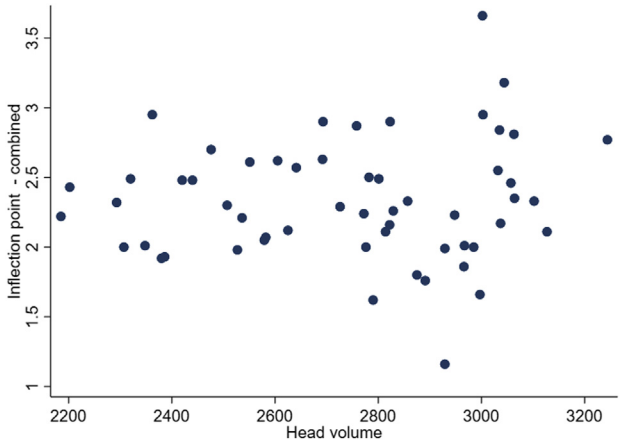

Figure 5. Scatterplot of the head volume versus the inflection point (subthalamic nucleus [STN] border location). The surgeon's judgment of the location of the STN border within the allocated 4-mm measured region was at 2 mm; the *dots* represent the objective measurements of the border location. Some dots outside the region of 0–4 mm (from magnetic resonance imaging scans with linear graphs; $n = 9$) were not depicted in this visual representation. No statistically significant difference was found between the accuracy of the surgeon's judgment of the STN border location and an increasing head volume.

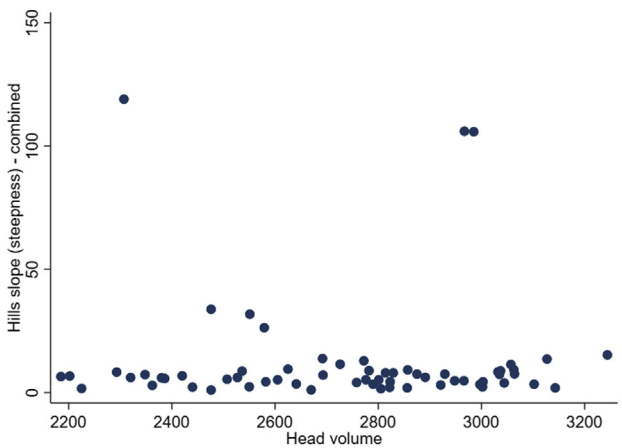

Figure 6. Scatterplot of the head volume versus the Hill slope (subthalamic nucleus border clarity). No statistically significant difference was found between an increasing head volume and changes in the Hill slope.

Table 3. Summary of Existing Qualitative Assessment Methods

Investigator	Method
Dimov et al.,[7] 2018	5-Point scale: 0 (STN border not visible) to 4 (all borders clearly defined, with an intensity gradient along the STN toward its caudal pole visible)
Ranjan et al.,[8] 2018	4-Point scale: 0 (STN border not visible) to 3 (excellent, with STN boundary visible and definitely clear)
Nagahama et al.,[9] 2015	4-Point scale: 0 (STN border not visible) to 3 (excellent, with STN boundary visible and definitely clear)
Liu et al.,[10] 2013	4-Point scale: 0 (STN border not visible) to 3 (STN well-defined and clearly differentiated from its superior neighbor [ZI] and inferior neighbor [SN])

STN, subthalamic nucleus; ZI, zona incerta; SN, substantia nigra.

border is poorly defined, a line, rather than a sigmoid curve, will be generated.

Comparison with Other Visualization Scores

Our method provides a novel and simple quantitative assessment of the quality or usability of an MRI scan for the visualization of the STN for DBS, providing an objective measure of the STN border location and clarity. Previous groups have described qualitative assessment of the STN and its borders using ordinal scales (Table 3).[7-10] However, the subjective nature of these scales has been a major shortcoming that could impair reliable replication by other investigators.

Quantitative assessment of the visibility of the STN has also been described using CNRs. The mean intensity value of voxels within a nominated STN region of interest is compared with the mean value of voxels of the surrounding tissue and set against various definitions of image noise (Table 4).[7,9-11] These offer an improved objective method; however, the interpretation is not particularly intuitive and the definition of CNR has varied in reported studies. Furthermore, the values provide a measure of the mean contrast of a structure relative to its neighbor, rather than specific information of the contrast at the border, which is the region of most interest to DBS surgeons.

Table 4. Summary of Existing Quantitative Assessment Methods

Investigator	Method
Dimov et al.,[7] 2018	CNR: $(ROI_{STN} - ROI_{WM})/SD_{WM}$ (STN divided into quadrants, with signal intensity measured within a ROI inside and outside the STN, divided by the SD of the intensity within the adjacent WM)
Alkemade et al.,[11] 2017	CNR: $(ROI_{inside\ STN} - ROI_{outside\ STN})/SD_{outside\ STN}$
Nagahama et al.,[9] 2015	CNR: $(ROI_{STN} - ROI_{SN})/SD_{STN}$ (coronal imaging used)
Liu et al.,[10] 2013	CNR: $(ROI_{inside\ STN} - ROI_{outside\ STN})/SD_{thalamus}$

CNR, contrast/noise ratio; ROI, region of interest; STN, subthalamic nucleus; WM, (adjacent) white matter; SD, standard deviation; SN, substantia nigra.

Application of Sigmoid Function Technique

Use of the sigmoid curve in the present report demonstrated that a larger head volume (measuring the supratentorial compartment, including the skull and scalp) did not result in poorer visualization of the STN. Until now, according to our literature search, no other study has specifically addressed such a hypothesis. The closest study was reported by Ranjan et al.,[8] who found that a lower volume of white matter correlated with poorer STN visualization using fast spin echo inversion recovery MRI. White matter atrophy correlates with age. Also, other studies have reported that the STN volume and neuron count will decline with age[12]; thus, this observation was related to a different clinical phenomenon. It is an interesting observation, nevertheless, because it is apparently in contrast to intuition from the reported data, which have documented a progressive increase in the iron concentration in other nuclei of the basal ganglia (and, therefore, presumably better delineation on T2-weighted MRI).[3]

Understanding the factors affecting visualization could support future research and guide imaging advances. On a day-to-day basis, it might also prompt the neurosurgeon in the preoperative setting, especially one who relies wholly on image guidance, to consider other targeting methods or to choose a different DBS target in the appropriate setting, such as the globus pallidus interna or the ventral intermedius nucleus. Although in our study, the sigmoid curve was determined with reference to the surgeon's judgment of the border location, the corollary is also possible during preoperative planning (i.e., if an STN border appears indistinct, voxels taken along the border region could be graphed to aid in a best estimate of its location). Although the sigmoid function method described in our concept study was not used to map the posterior STN border preoperatively per se, future studies in which the technique is primarily used should consider incorporating a method to assess and verify final lead placement accuracy (e.g., through correlation with clinical response).

CONCLUSION

Similar to other quantitative tools, the novel application of the sigmoid curve function allows for an objective assessment and, therefore, comparison of MRI scans for DBS. It is conceptually simple with potential utility in both the clinical and the academic setting. We used the sigmoid curve to demonstrate that the head volume does not adversely affect STN image quality on high-resolution T2-weighted MRI scans.

CRediT AUTHORSHIP CONTRIBUTION STATEMENT

Anthony M.T. Chau: Conceptualization, Methodology, Investigation, Formal analysis, Writing - original draft, Writing - review & editing, Visualization. **Angela Jacques:** Formal analysis, Visualization. **Christopher R. Lind:** Conceptualization, Methodology, Resources, Writing - review & editing, Supervision.

ACKNOWLEDGMENTS

The authors thank Professor Max K. Bulsara, Chair, Department of Biostatistics, University of Notre Dame, for his advice.

REFERENCES

1. Kocabicak E, Alptekin O, Ackermans L, et al. Is there still need for microelectrode recording now the subthalamic nucleus can be well visualized with high field and ultrahigh MR imaging? *Front Integr Neurosci*. 2015;9:46.

2. Yelnik J. Functional anatomy of the basal ganglia. *Mov Disord*. 2002;17:S15-S21.

3. Dormont D, Ricciardi KG, Tande D, et al. Is the subthalamic nucleus hypointense on T2-weighted images? A correlation study using MR imaging and stereotactic atlas data. *AJNR Am J Neuroradiol*. 2004;25:1516-1523.

4. Güngör A, Baydin ŞS, Holanda VM, et al. Microsurgical anatomy of the subthalamic nucleus: correlating fiber dissection results with 3-T magnetic resonance imaging using neuronavigation. *J Neurosurg*. 2018;130:716-732.

5. Thani NB, Bala A, Lind CR. Accuracy of magnetic resonance imaging-directed frame-based stereotaxis. *Neurosurgery*. 2012;70:114-123.

6. Schaltenbrand G, Wahren W. *Atlas for Stereotaxy of the Human Brain*. New York, NY: Thieme Medical Publishers; 1977.

7. Dimov AV, Gupta A, Kopell BH, Wang Y. High-resolution QSM for functional and structural depiction of subthalamic nuclei in DBS presurgical mapping. *J Neurosurg*. 2018;131:360-367.

8. Ranjan M, Boutet A, Xu DS, et al. Subthalamic nucleus visualization on routine clinical preoperative MRI scans: a retrospective study of clinical and image characteristics predicting its visualization. *Stereotact Funct Neurosurg*. 2018;96:120-126.

9. Nagahama H, Suzuki K, Shonai T, et al. Comparison of magnetic resonance imaging sequences for depicting the subthalamic nucleus for deep brain stimulation. *Radiol Phys Technol*. 2015;8:30-35.

10. Liu T, Eskreis-Winkler S, Schweitzer AD, et al. Improved subthalamic nucleus depiction with quantitative susceptibility mapping. *Radiology*. 2013;269:216-226.

11. Alkemade A, de Hollander G, Keuken MC, et al. Comparison of T2*-weighted and QSM contrasts in Parkinson's disease to visualize the STN with MRI. *PLoS One*. 2017;12:e0176130.

12. Zwirner J, Mobius D, Bechmann I, et al. Subthalamic nucleus volumes are highly consistent but decrease age-dependently—a combined magnetic resonance imaging and stereology approach in humans. *Hum Brain Mapp*. 2017;38:909-922.

Conflict of interest statement: The authors declare that the article content was composed in the absence of any commercial or financial relationships that could be construed as a potential conflict of interest.

Received 7 July 2020; accepted 3 August 2020

Citation: World Neurosurg. (2020). https://doi.org/10.1016/j.wneu.2020.08.027

*Journal homepage: **www.journals.elsevier.com/world-neurosurgery***

*Available online: **www.sciencedirect.com***